International Journal of Biochemistry and Cell Biology 116 (2019) 105599

Contents lists available at ScienceDirect

International Journal of Biochemistry and Cell Biology

journal homepage: www.elsevier.com/locate/biocel

Alternative isoforms of BmYki have different transcriptional co-activator activity in the silkworm, Bombyx mori

Zi Liang[a,c], Yahong Lu[a,c], Mengsheng Jiang[a,c], Ying Qian[a,c], Liyuan Zhu[a,c], Sulan Kuang[a,c], Fei Chen[a,c], Yongjie Feng[a,c], Xiaolong Hu[a,b], Guangli Cao[a,b], Renyu Xue[a,b,*], Chengliang Gong[a,b,c,*]

[a] School of Biology & Basic Medical Science, Soochow University, Suzhou, 215123, China
[b] National Engineering Laboratory for Modern Silk, Soochow University, Suzhou, PR China
[c] Agricultural Biotechnology Research Institute, Agricultural biotechnology and Ecological Research Institute, Soochow University, Suzhou, 215123, China

ARTICLE INFO

Keywords:
Bombyx mori
Hippo pathway
Yorki
Alternative splicing
Transcriptional co-activator

ABSTRACT

Yorki (Yki), a transcriptional co-activator that is a key component of the Hippo pathway, induces the transcription of a number of targets that promote cell proliferation and survival. *Bombyx mori* Yki3 (BmYki3), with 445 amino acid residues, facilitates cell migration and cell division, and enlarges cultured cell and wing disc size. In this study, cellular localization, transcriptional co-activator activity, cell migration, cell cycle, and cell size were characterized in alternative isoforms of BmYki. BmYki1 and BmYki3 are mainly located in the cytoplasm and nucleus, respectively, while, BmYki2 is located in both the cytoplasm and nucleus. The mutation BmYki1^{S97A} (S^{97}mutated to A) was transported from the cytoplasm to nucleus. Cell migration, cell cycle, and cell size could be enhanced by BmYki, however, the effect of BmYki1 and BmYki2 on cell proliferation was less compared to BmYki3. Moreover, wing discs could be enlarged by overexpressing BmYki1 or BmYki2 isoforms. Dual-luciferase reporter assay showed that BmYki3 had the highest activity to *B. mori* ovarian tumor gene. In BmN cells overexpressing one of the BmYki isoforms, expression levels of kibra ortholog (*kibra*), inhibitor of apoptosis protein (*iap*), four-jointed (*fj*), expanded (*ex*), crumbs (*crb*) and BMP and activin membrane-bound inhibitor homolog (*Bmpr*) genes were upregulated, while those of α-catenin (*α-cat*), decapentaplegic (*dpp*), serrate (*serr*) and signal transducer and activator of transcription (*stat*) genes were down-regulated. There was some difference in the regulation of gene expression between different isoforms. These results suggested that the activity of BmYki isoforms was different in the silkworm.

1. Introduction

The Hippo pathway is an important signaling pathway for the regulation of organ growth (Madhuri and Amit, 2009; Stocker and Hafen, 2000; Edgar, 2006; Pan, 2007). The core components in the Hippo pathway consist of a series of phosphorylated proteins, including the serine/threonine Ste20 kinase Hippo (Hpo) (Wu et al., 2003; Jia et al., 2003), nuclear Dbf-2 related (NDR) family kinases Warts (WTS), a scaffold protein salvador (sav) (Harvey et al., 2003; Pantalacci et al., 2003; Udan et al., 2003), and mob-as-tumor-suppressor (mats) (Lai et al., 2005; Wei et al., 2007). In our previous study, the *Hpo*, *Sav*, *Mats*, and *Wts* genes related to the Hippo pathway in the silkworm were identified (Qian et al., 2013). Although the sequence identities of the proteins from different species were not high, the conserved domains were prominent (Qian et al., 2013), suggesting that the Hippo pathway was evolutionarily conserved. Any component in the pathway that is abnormally expressed or mutated will result in abnormal growth. For example, during the imaginal development of the fruit fly *Drosophila melanogaster*, the *Wts* mutant will give rise to an excessive proliferation of cells in the development of multiple tissues. *Yorkie* (Justice et al., 1995; Huang et al., 2005) with a WW domain, is a downstream element of the *Wts–Mats* complex (Wu et al., 2003; Wei et al., 2007) which is activated by the phosphorylated *Hpo-Sav* complex (Huang et al., 2005). The activation of the *Wts–Mats* complex results in the phosphorylation of Yorkie (Yki), which is associated with the 14-3-3 protein in the cytoplasm, and is inactivated and retained in the cytoplasm (Ren et al., 2010; Zhang et al., 2008). When the Hippo signaling pathway is inhibited, Yki is transferred into the nucleus and combined with the transcription factor *Sd* (Zhang et al., 2008; Goulev et al., 2008; Wu et al., 2008; Zhao et al., 2008; Nolo et al., 2006), which up-regulates the

* Corresponding author at: School of Biology & Basic Medical Science, Soochow University, Suzhou, 215123, China.
E-mail addresses: xuery@suda.edu.cn (R. Xue), gongcl@suda.edu.cn (C. Gong).

https://doi.org/10.1016/j.biocel.2019.105599
Received 29 May 2019; Received in revised form 2 September 2019; Accepted 4 September 2019
Available online 05 September 2019
1357-2725/

expression of target genes, including *diap1*, *cyclinE*, and *Bantam*, to finally result in cell proliferation and the inhibition of apoptosis (Thompson and Cohen, 2006; Campbell et al., 1992). Therefore, Yki is an important transcriptional co-activator. A previous study indicated that the serine-threonine-like kinase protein Hpo, WW-domain-containing adaptor protein Sav, Mats, NDR family kinase protein Wts, and transcriptional co-activator Yki were genes related to the Hippo pathway in the silkworm (Qian et al., 2013). Smaller body size and late-stage larval lethality in the silkworm, *Bombyx mori*, could be induced by the *B. mori* Hpo (BmHPO) mutation (Xu et al., 2018a). Cell proliferation activity and the cell cycle were changed with the up-regulation and de-regulation of *BmHPO* (Li et al., 2018).

In our previous study, the cDNA of three *B. mori Yki* (BmYki) isoforms encoding 437 (BmYki1, AHJ26002.1), 390 (BmYki2, AHJ26003.1), and 445 (BmYki3, AHJ26004.1) amino acid residues were identified (Qian et al., 2013). BmYki1 was weakly expressed in the tissues assessed, and the lowest level was in the silk gland. BmYki2 expressed highest in the head. BmYki3 expressed highest in the silk gland, and was weakly expressed in the haemocyte (Liang et al., 2018). Moreover, another isoform with 395 amino acid residues was found (Zeng et al., 2018). The results reported by Liu et al. indicated that BmYki1 potentially facilitates posterior silk gland growth and metamorphosis in the silkworm (Liu et al., 2016), moreover, it was found that the weight of the posterior silk gland, cocoon, larval body, and pupal body could be increased by overexpressing Yorki^{CA} (Ser^{97} of the BmYki1 was mutated to Ala^{97}) (Zhang et al., 2017).

Body size, molting defects and, eventually, larval lethality could be induced by knocking out BmYki (Xu et al., 2018b). Our previous results indicated that cultured cells and wing disc size of the silkworm can be controlled by BmYki3 (Liang et al., 2018).

Many genes in the eukaryotic genome are alternatively spliced to form multiple transcripts. It was reported that a gene could generate multiple transcripts encoding proteins with differing or opposing functions, and a large majority of predicted alternative transcripts may not even be translated into proteins (Bates et al., 2017). In Drosophila, the *Ovo* locus encodes three isoforms, Shavenbaby (Svb), OVO-A and OVO-B (Garfinkel et al., 1994), but their expression pattern and finctions were quite different (Garfinkel et al., 1994; Lee and Garfinkel, 2000). In generally, although a lot of alterative splicing isoforms were found, very few alternative protein isoforms have well-characterized cellular function.

In the present study, we characterized the cellular location of BmYki isoforms and compared the effect of overexpressing BmYki on cell migration, cell cycle, cell size, and target gene expression. Our results suggest that alternative isoforms of BmYki have a different transcriptional co-activator activity, the impact of BmYki3 on the regulation of migration, cell cycle, and size of cells was the greatest among the three BmYki isoforms.

2. Materials and methods

2.1. Construction of recombinant plasmids overexpressing BmYki

The cDNA of two BmYki isoforms encoding 437 (BmYki1, AHJ26002.1) and 390 (BmYki2, AHJ26003.1) amino acid residues were subcloned into the KpnI/EcoRI sites of the pIZT/V5-His vector (Invitrogen, Frederick, MD, USA) to generate recombinant plasmid pIZT/V5-His-BmYki1 and pIZT/V5-His-BmYki2, respectively. A recombinant plasmid Pizt/V5-His-BmYki3 containing the cDNA sequence of BmYki3 (BmYki3, AHJ26004.1) with 443 amino acid residues was constructed in our previous study (Liang et al., 2018).

The serine at residue 168 (S^{168}) in Drosophila Yki is a phosphorylation site (Ren et al., 2010). Bioinformation analysis indicated that BmYki1 S^{97} maybe a phosphorylation site because BmYki1 S^{97} corresponds to the Drosophila Yki S^{168}. To mutate the S^{97} to alanine (A), the codon TCG (289–291 nt) of S^{97} in BmYki1 was replaced with codon GCT. The mutated BmYki1 (BmYki1^{S97A}), which was confirmed by sequencing, was cloned into pIZT/V5-His to generate pIZT/V5-His-BmYki1^{S97A}.

2.2. Construction of the fluorescent reporter vector

To generate the luciferase expression vector, the promoter of the *B. mori* ovarian tumor (*Bmotu*) amplified from silkworm genomic DNA (*Dazao* strain) with the primers Potu5/Potu2-1 (Table S1) was cloned into the SmaI and BamHI sites of a pFastBac™Dual vector (Frederick, MD, USA) to generate pFast-potu5. The luciferase gene (*luc*) amplified from plasmid pGL3 (Frederick, MD, USA) with the primers Luc1/Luc2 (Table S1) was inserted into the KpnI and SmaI sites of pFast-potu5 to obtain the vector pFast-potu5-Luc.

2.3. Cell culture, transfection, and transformed cells

The BmN cell line derived from *B. mori* ovary was cultured in TC-100 (Gibco BRL, Rockville, MD, USA) supplemented with 10% fetal bovine serum (FBS) at 26.5 °C. Transfection of BmN cells with recombinant plasmids overexpressing BmYki was carried out using DNA Transfection Reagent (Roche Diagnostics, Mannheim, Germany) following the manufacturer's protocol. At 3 days after transfection, the cells were screened continuously for a month with zeocin, at a final concentration of 200 μg/mL, to generate BmN-Yki1, BmN-Yki2, BmN-Yki3, and BmN-BmYki1^{S97A} transformed cells. Simultaneously control transformed cells (BmN-null) were generated by transfecting pIZT/V5-His into BmN cells and screened with zeocin.

2.4. Luciferase reporter assay

Reporter activity was determined using the Dual-Luciferase Reporter Assay System (Promega, Madison, WI, USA) according to the manufacturer's instructions. A mixture of pFast-potu5-Luc (1 μg), pRL-TK (0.1 μg), and pIZT/V5-His-BmYki (10^{11} copies) plasmids were transfected into BmN cells (1×10^5), and BmN cells co-transfected with pFast-potu5-Luc, pRL-TK, and pIZT/V5-His plasmids were used as a control. At 60 h post-transfection, BmN cells were collected and lysed for 15 min at room temperature using 1 × passive lysis buffer (Promega, Madison, WI, USA), and then the lysed cells were centrifuged at 12,000 *g*for 10 min. The supernatant was used for the determination of luciferase activity. Luciferase activity was measured using GloMax Multi Jr at 490 nm (Promega, Madison, WI, USA).

2.5. Immunofluorescent staining

BmN cells were collected and fixed with 4% paraformaldehyde for 15 min, then rinsed with 0.01 M of PBST (0.05% of Tween-20 in PBS) and incubated with the prepared mouse anti-BmYki1 antiserum (Liang et al., 2018) at 4 °C overnight. At the same time, BmN cells were incubated with pre-immune antiserum as a negative control. After rinsing with 0.01 M PBST three times, the cells were incubated with TRITC-conjugated goat anti-mouse IgG (Tiangen, Beijing, China) at 37 °C for 1 h. After removing non-combined TRITC-conjugated goat anti-mouse IgG and staining with DAPI, the cells were then observed by an inverted microscope (TE2000U, Nikon, Japan).

2.6. Cell wound healing assay

Cells (5×10^5) were added to a six-well plate and cultured overnight. A scratch wound was made across each well of the six-well plate using a pipette tip. The plates were washed three times with PBS to remove any loosely held cells and to ensure that the wound area was free of cells. FBS free TC-100 medium was added and the cells were cultured at 26.5 °C. Images were taken every 6–12 h post-scratch to determine the speed of cell migration. ImageJ (https://imagej.nih.gov/

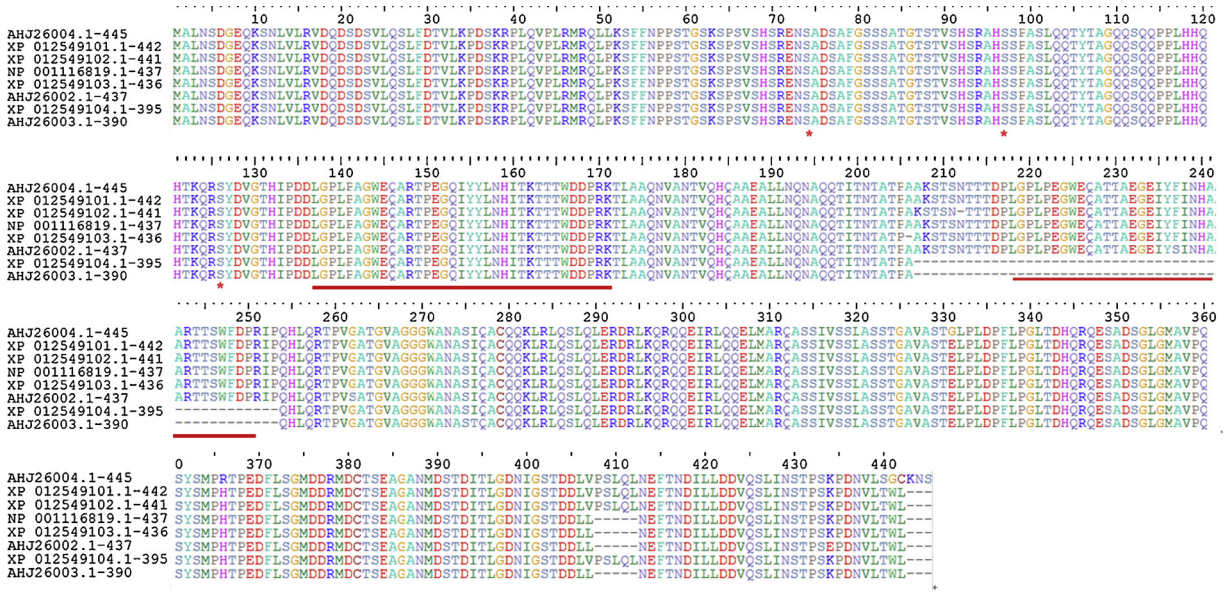

Fig. 1. Alignment of the deposited BmYki isoforms of silkworm in GenBank and the deduced phosphorylation sites. 'S' amino acid residue marked with an asterisk was a deduced phosphorylation site, amino acid residue marked with an underline was WW domain. In this study, BmYki with 437 (AHJ26002.1), 390 (AHJ26003.1) and 445 (AHJ26004.1) amino acid residues respectively are termed as BmYki1, BmYki2 and BmYki3.

ij/) were used to calculate the scratch distance according to the process.

2.7. Cell proliferation

BmN cells (2×10^5/mL, 2 mL) were added to a culture flask. After adherent culture for 24 h, cells were observed under a microscope and images were taken of five fixed views every 24 h to determine the cell number in each view. ImageJ were used to count the cell number in the captured images.

2.8. Cell size

Cells (1×10^6) were transfected with either pIZT/V5-His-BmYki1, pIZT/V5-His-BmYki2, pIZT/V5-His-BmYki3 (Garfinkel et al., 1994), or pIZT/V5-His. After 24 h, the size of cells with and without fluorescence were assessed every 24 h in the same culture.

2.9. Flow cytometer

To assess the effect of BmYki on the cell cycle, the ratios of cells at G1, S, and G2 phases were estimated by flow cytometer according to our previous report (Liang et al., 2018).

2.10. Real-time quantitative-PCR

Total RNAs were extracted from the cultured cells by using a High Pure RNA Isolation Kit (Roche, Indianapolis, USA). The total RNA (1 μg) was reverse-transcribed with a First-Strand cDNA Synthesis Kit (TaKaRa, Dalian, China). Real-time PCR was carried out with a real-time reverse transcription-PCR system (Cycler 1000; Bio-Rad, Hercules, CA, USA) with SYBR green. The *B. mori* housekeeping gene *actin* A3 was used as an internal control for normalization. The mixture (20 μL) included 2 μL of cDNA, 0.5 μL of each primer (10 mM), 10 μL of SYBR Premix ExTaq (Bio-Rad, Hong Kong, China) and 6 μL ddH2O. Real-time PCR was carried out as follows: one cycle at 50 °C for 2 min, one cycle at 95 °C for 10 min, 40 cycles at 95 °C for 15 s and 60 °C for 1 min, with a final cycle at 95 °C for 15 sec, 60 °C for 30 sec and 95 °C for 15 s. Relative gene expression was estimated according to the $2^{-\Delta\Delta Ct}$ method. All samples were run in triplicate. The experimental data were statistically analyzed using the Student's t-test. A value of $P < 0.05$ was considered significant. The primers used in the present study are listed in Table S1.

2.11. Overexpressing the BmYki gene in wing discs

Our previous study indicated that BmYki3 could enlarge wing disc size (Liang et al., 2018). To assess the effect of up-regulating the *BmYki1* or *BmYki2* gene expression level in the wing disc, 10 pupae at day 3 pupation were injected with pIZT/V5-His-BmYki1 or pIZT/V5-His-BmYki2 below the right-wing disc (1 μg/μl, 2 μl, per pupa). The negative controls (the left-wing disc) were injected with water (2 μl, per pupa).

3. Results

3.1. BmYki has seven alternative splicing isoforms at least

Multiple transcripts derived from a gene can be generated by alternative splicing in the eukaryon. In our previous study, three BmYki isoforms termed BmYki1, BmYki2, and BmYki3, encoding 437 (AHJ26002.1), 390 (AHJ26003.1), and 445 (AHJ26004.1) amino acid residues, respectively, were cloned and sequenced (Qian et al., 2013). To further detect the transcripts of *BmYki*, BlastN was carried out with *BmYki* gene sequences, five other transcripts encoding 442 (XP_012549101.1), 441 (XP_012549102.1), 436 (XP_012549103.1), 395 (XP_012549104.1) and 437 (NP_001116819.1) amino acid residues were found. The amino acid sequence alignment result is displayed in Fig. 1.

A search for conserved domains indicated that there was a FAM181 (region 35–143) in all the isoforms; the AHJ26002.1, AHJ26004.1, XP_012549103.1, XP_012549102.1, XP_012549101.1 and NP_001116819.1 isoforms contained a 2 W W domain (Domain with two conserved Trp residues) which can bind proline-rich polypeptides (Chen and Sudol, 1995), while AHJ26003.1 and XP_012549104.1 had a WW domain. It was reported that Drosophila Yki S^{111}, S^{168}, and S^{250} were phosphorylation sites (Ren et al., 2010). Bioinformatics analysis showed that BmYki1 S^{74}, S^{97}, and S^{126} were phosphorylation sites (Fig. 1).

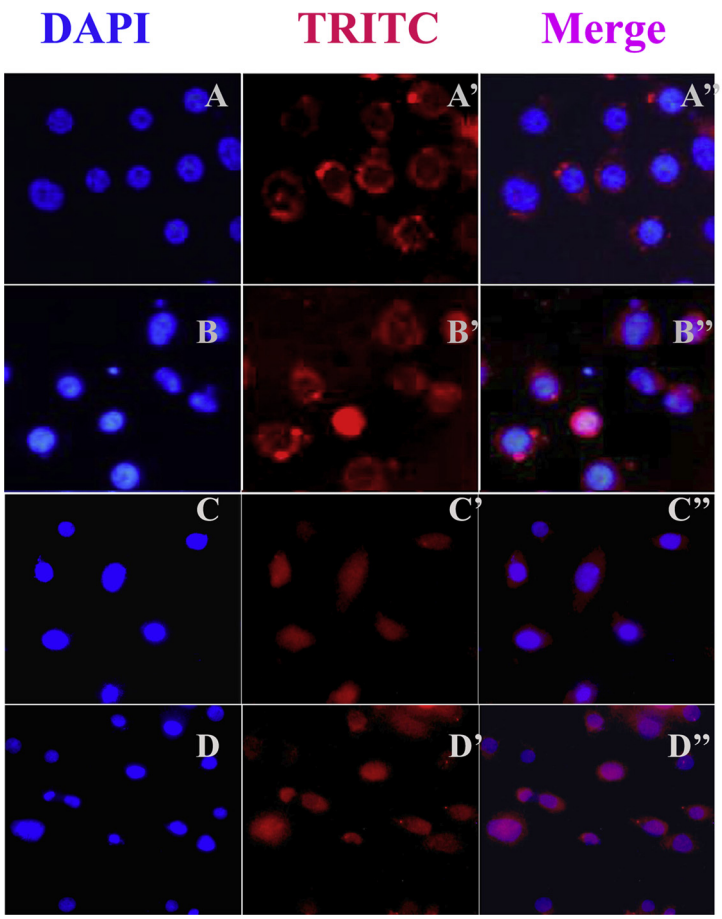

Fig. 2. The sub-cellular location of BmYki isoforms in their corresponding transformed cells. (Magnification: 10 × 40). A, A', A": BmN-Yki1 ; B, B', B": BmN-Yki1^{S97A} ; C, C', C" : BmN-Yki2; D, D', D" : BmN-Yki3; A, B, C, D: the nucleus was stained with DAPI (blue); A', B', C', D': the BmYki was stained with TRITC; A", B", C", D": merged A, B, C, D and E respectively with A', B', C', D'and E'.

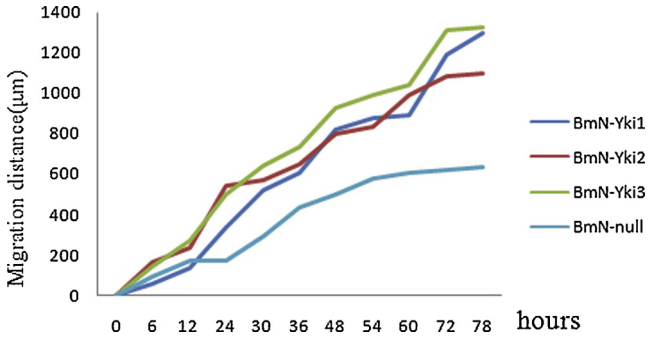

Fig. 3. Comparison of cell migration among the different transformed cells. BmN-null, BmN-Yki1, BmN-Yki2 and BmN-Yki3 represented the transformed cells respectively with pIZT/V5-His, pIZT /V5-His-BmYki1, pIZT/V5-His-BmYki2 and pIZT/V5-His-BmYki3. Cell wound healing assay was used to assess cell migration, the migration distance was measured every 6 h.

3.2. Transport of BmYki to the nucleus is promoted by mutating the S^{97} residue of BmYki to alanine (A)

Our previous study showed that BmYki was mainly located in the nucleus of cultured BmN cells (Liang et al., 2018). To understand the cellular location of BmYki isoforms and the effect of BmYki phosphorylation on cellular location, BmN cells were transfected with either pIZT/V5-His, pIZT/V5-His-BmYki1, pIZT/V5-His-BmYki2, pIZT/V5-His-BmYki3, or pIZT/V5-His-BmYki1^{S97A} and screened continuously for more than a month with zeocin to generate BmN-null, BmN-Yki1, BmN-Yki2, BmN-Yki3 (Liang et al., 2018), and BmN-BmYki1^{S97A} transformed cells. The qPCR results indicated that the corresponding *BmYki* gene expression level was upregulated in the transformed cells. Immunofluorescence assay showed that BmYki1 was mainly distributed in the cytoplasm in the transformed cells BmN-BmYki1 (Fig. 2A, A′, A″), whereas BmYki1 was found to be located in the nucleus of cells transformed with BmN-BmYki1^{S97A} (Fig. 2B, B′, B″). Drosophila Yki S^{168} is a critical Wts phosphorylation site (Oh and Irvine, 2009), bioinformatic analysis indicated that BmYki1 S^{97} corresponded to Drosophila Yki S^{168}. Our results indicated that the transport of BmYki to the nucleus was promoted by mutating the BmYki1 S^{97} to A, suggesting BmYki1 S^{97} was also a Wts phosphorylation site. Moreover, we also found that BmYki was distributed in both cytoplasm and nucleus in BmN-BmYki2 cells (Fig. 2C, C′, C″) and mainly located in the nucleus of BmN-BmYki3 transformed cells (Fig. 2D, D′, D″), suggesting that distribution and location of BmYki in the cells could be also determined by unknown factors in addition to the phosphorylation of BmYki.

3.3. Cell migration could be facilitated by different BmYki isoforms

To understand the effect of different BmYki isoforms on cell migration, a cell wound healing assay was carried out. The results showed that cells migration could be promoted by overexpressing the *BmYki* gene, the migration distance of BmN-BmYki1 and BmN-BmYki2 cells was less (Fig. 3) than that of BmN-BmYki3 cells (Liang et al., 2018).

3.4. Cell proliferation could be facilitated by different BmYki isoforms

Our previous study indicated that BmYki3 facilitates cell proliferation (Liang et al., 2018). To characterize the difference in the promotion of cell proliferation between BmYki isoforms, the cell number per view was investigated under a microscope. The initial value of cell number per view was similar between the different transformed cells, however, 9 days later, the cell number of BmN-BmYki1, BmN-BmYki2,

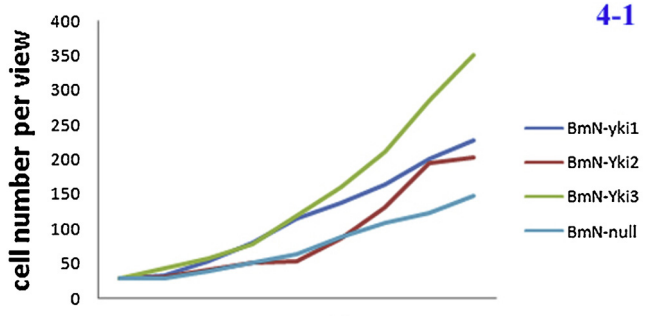

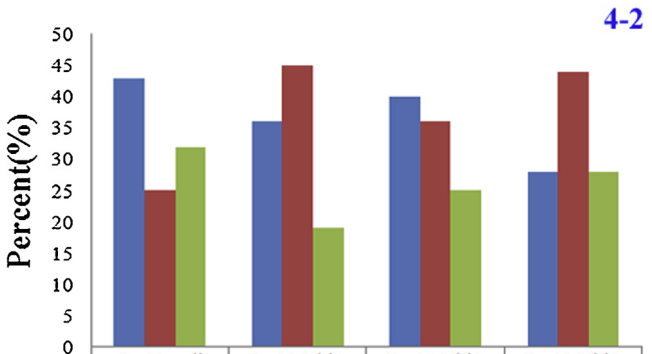

	BmN-null	BmN-Yki1	BmN-Yki2	BmN-Yki3
G1(%)	43	36	40	28
S(%)	25	45	36	44
G2(%)	32	19	25	28

Fig. 4. Comparison of cell proliferation among the different transformed cells. 4–1: The 2×10^5/mL of the transformed cells (2 mL) were added into a culture flask, after adherent culture for 24 h, 5 fixed views were selected, took image every 24 h to determine cells number per views. 4–2: The synchronized cells were cultured in TC-100 medium supplemented with 10% FBS for 48 h, the ratio of cells in G1, S and G2 phase for BmN-null, BmN-BmYki1, BmN-BmYki2 and BmN-Yki3 were respectively estimated by flow cytometer.

and BmN-null increased by 8.07, 7.14 and 5.29 folds, respectively, compared to the initial value, while the cell number of BmN-BmYki3 increased by 12.26-fold (Liang et al., 2018). This indicated that cell proliferation could be facilitated by BmYki, the proliferation rates for BmN-BmYki3 were fastest, followed by BmN-BmYki1, and then BmN-BmYki2 (Figs. 1–4). The ratio of G1, S, and G2 phases, which were estimated by flow cytometry after the synchronized cells were cultured in TC-100 medium supplemented with 10% FBS for 48 h, was used to assess cell proliferation. The results showed that the ratio of the G1, S, and G2 phase was 43%, 25%, and 32% in BmN-null transformed cells (Liang et al., 2018), 36%, 45%, and 19% in BmN-BmYki1 cells, and 40%, 36%, and 24% in BmN-BmYki2 cells, respectively (Figs. 2–4). This confirms that BmYki1 and BmYki2 could promote cell proliferation in the same way as BmYki3 (the ratio of G1, S, and G2 phase was 28%, 44% and 28% in BmN-BmYki3 transformed cells) (Figs. 2–4) (Liang et al., 2018).

3.5. BmYki could enlarge cell size

To assess the effect of different isoforms of BmYki on cell size, BmN cells were transfected with vectors overexpressing BmYki and the size of cells with/without fluorescence were investigated every 24 h. The results indicated that the size of transformed cells with fluorescence was larger than cells without fluorescence, indicating that BmYki could increase the cell size. An obvious difference in cell size was not found among different treatment groups (Fig. 5).

3.6. Expression of genes related to signaling pathways, the cell cycle, and apoptosis could be regulated by overexpressing BmYki

To further understand the role of BmYki isoforms on the regulation of cell size, cell division, and expression level of genes in related signaling pathways, the cell cycle, and apoptosis were investigated after *BmYki* was upregulated. The results showed that an obvious change was not found in the expression level of the *wts*2 gene, however, the expression level of genes upstream (*kibra*, *Fj* and *Ex*) of the Hippo pathway was upregulated. The expression level of the inhibitor of apoptosis protein (*iap*) and BMP and activin membrane-bound inhibitor homolog (*Bmpr*) genes, negative regulators of TGF-beta, were also upregulated after a *BmYki* gene was over-expressed in the cultured cells (Fig. 6); whereas, the *catenin alpha* (*cat*, function as a linking protein between cadherins and actin-containing filaments of the cytoskeleton), *decapentaplegic* (*dpp*, a member of the TGF-β superfamily), *serrate* (*serr*, a Notch ligand), signal transducer and activator of transcription (stat, JAK-STAT Pathway) genes were down-regulated. Comparison analysis indicated that there were some differences in the regulation effectiveness of different BmYki isoforms on the genes tested (Fig. 6).

3.7. The activity of the Bmotu gene promoter could be increased by BmYki3

Yki functions as a co-activator, after being transported into the nucleus, which could interact with transcriptional factor Scalloped (sd) and promoted target gene expression. To assess the activity of different BmYki isoforms, the activation effect of BmYki to the *Bmotu* gene promoter was investigated with a dual-fluorescence reporter assay, the results showed that the activity of the promoter could be facilitated only by BmYki3 (Fig. 7). Compared to the other isoforms, BmYki3 has an extra amino acid sequences 'PSLQL', which could be involved in the promotion of *Bmotu* gene promoter activity.

3.8. Both BmYki1 and BmYki2 could enlarge wing disc size

Wing disc size could be enlarged by BmYki3 (Liang et al., 2018). To assess the effects of up-regulating the *BmYki1* or *BmYki*2 gene on the development of the wing disc, the right and left wing discs of 10 pupae were injected with pIZT/V5-His-BmYki1 or pIZT/V5-His-BmYki2 and water, respectively. Approximately 30% (20%) of the front wing was increased by 13.3–25% (16.7–20%) and approximately 20% (20%) of the hind wing was increased by 11.1–12.5% (12.5–25%) in length in the group injected with pIZT/V5-His-BmYki1(pIZT/V5-His-BmYki2), whereas the abnormal wing was not observed in the group injected with water. These results indicated that both BmYki1 and BmYki2 could enlarge the wing disc size (Table 1, Fig. 8).

4. Discussion

In the eukaryon, multiple mature mRNA can be generated from precursor mRNA via alternative splicing events. It has been an important way of extending the genetic information of a gene, but the functional role of alternative protein isoforms has been the subject of considerable debate. At the other extreme, it was considered that most alternative transcripts will not encode proteins, and alternative splicing may not be the key to the proteome complexity (Tress et al., 2007). A previous study has indicated that *BmYki* is transcribed into four functional splicing isoforms in the silk glands of the silkworm (Zeng et al., 2018). In this study, we found that eight spliced isoforms potentially coding 437, 442, 436, 441, 445, 390, 437 and 395 amino acid residues could be generated from *BmYki* precursor mRNA. Western blot analysis showed that two special signaling bands (about 50 and 43 kDa) representing BmYki could be observed in the testis, silk gland, and fat body (Liang et al., 2018), suggesting that some spliced isoforms of *BmYki* could translate into proteins. The S^{111}, S^{168}, and S^{250} in Drosophila Yki were phosphorylated by Wts, of which the S^{168} is most critical

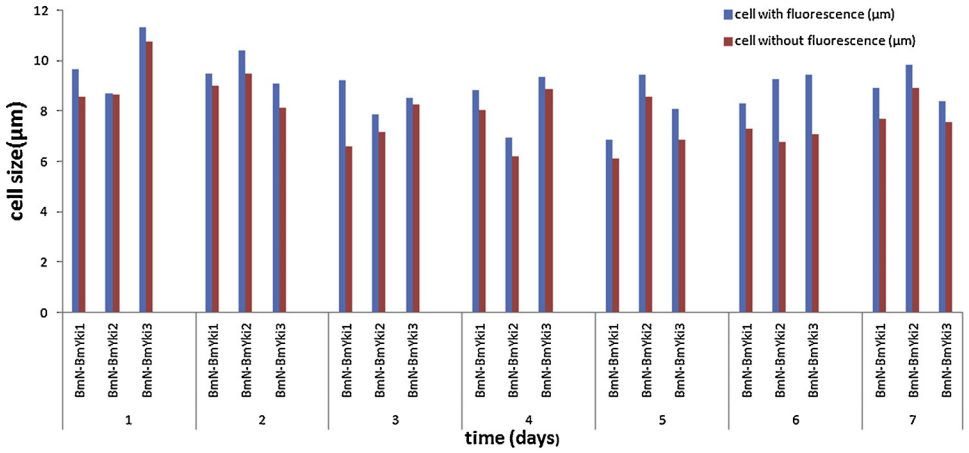

Fig. 5. Comparison of cell size for different transformed cells. The BmN cells were transfected with pIZT/V5-His-BmYki*1,* pIZT/V5-His-BmYki2 and pIZT/V5-His-BmYki3, respectively, the cells with/without fluorescence were measured every day.

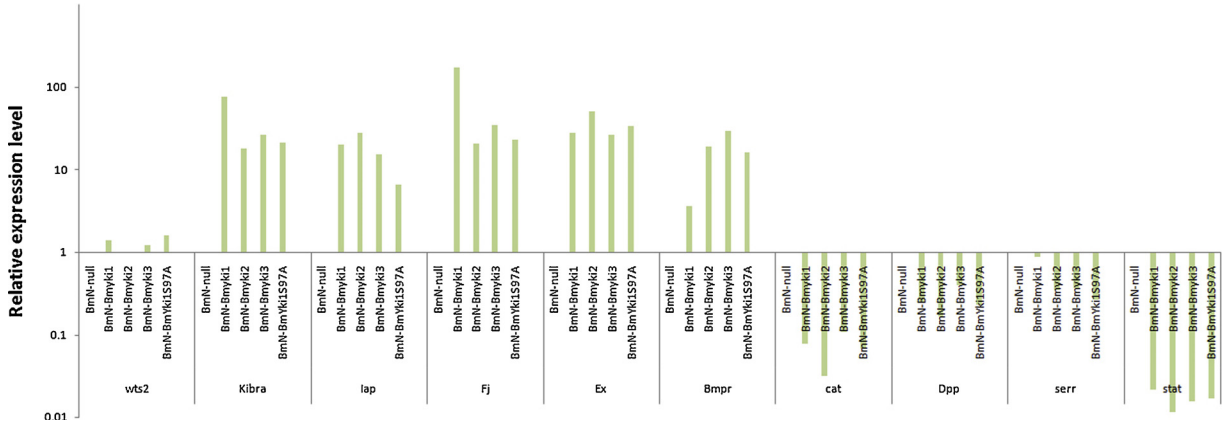

Fig. 6. Change in expression level of genes related signaling pathway, cell cycle and apoptosis after *BmYki* gene expression was up-regulated.

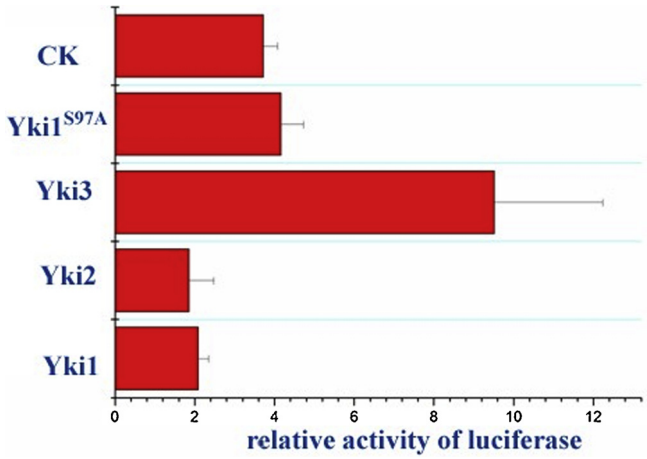

Fig. 7. Effect of BmYki isoforms on activity of *otu* gene promoter. The mixture of pFast-potu5-Luc (1 μg), pRL-TK (0.1 μg) and Pizt/V5-His-BmYki (10^{11} copies) plasmids were transfected into BmN cells (10^5), and the co-transfected BmN cells with pFast-potu5-Luc, pRL-TK and Pizt/V5-His plasmids was used as a control.The collected BmN cells at 60 h post-transfection were lysed, the supernatant (100 μg protein) was used for the determination of luciferase activity.

for interaction with the14-3-3 protein in the cytoplasm, and is inactivated and retained in the cytoplasm (Ren et al., 2010; Zhang et al., 2008). Bioinformatics analysis indicated that BmYki S^{74}, S^{97}, and S^{126} were phosphorylation sites. Subcellular location indicated that BmYki1 was transported from the cytoplasm into the nucleus after S^{97} was mutated to A, suggesting S^{97} phosphorylation contributes to the cellular location of BmYki1, which may be helpful in promoting cell migration and cell cycle, it may also increase cell size. Moreover, in the transformed cells BmN-BmYki1, BmYki was mainly located in the cytoplasm; in the transformed cells BmN-BmYki2, BmYki was located in both the cytoplasm and nucleus, while in the transformed cells BmN-BmYki3, BmYki was mainly located in the nucleus, suggesting there were some differences in the cellular location of BmYki isoforms. It was reported that there are some potential sites of phosphorylation by an unknown kinase in Drosophila Yki, which influence phosphorylation of S^{168} by Wts, suggesting that the cellular location of BmYki isoforms maybe also influenced by some unknown phosphorylation sites. Drosophila Yki protein has a WW domain which interacts with proline-rich polypeptides (Chen and Sudol, 1995). Yki associates with Wts via a WW domain PPXY motif interaction (Huang et al., 2005), whereas WW domains were not required for phosphorylation of Yki by Wts (Oh and Irvine, 2008) and for interaction with Sd, but instead are positively required for its activity (Oh and Irvine, 2009). Both BmYki1 and BmYki3 had two WW domains, whereas BmYki2 only had one. The WW domain binds to proteins with a particular proline-motif and/or a phosphoserine or phosphothreonine-containing motif, suggesting the activity of the transcriptional co-activation of BmYki isoforms were different. This speculation was confirmed by an investigation of the changes in some gene expression levels in the cultured cells after different *BmYki* isoforms were over-expressed.

It was hypothesized that alternative splicing exists to allow the tissue-specific rewiring of protein–protein interaction networks (Colak et al., 2013). In 14,623 predicted proteins of the silkworm, nearly 18%

Table 1
Effects of up-regulation of BmYki1 or BmYki2 gene expression on the size of the wing disc. Serial numbers 1–3 (4–6), at day 3 of pupation, the pupae were, respectively, injected with water for left wing disco and pIZT/V5-His-BmYki1(pIZT-V5/His-BmYki2) for right wing disco.

Serial number	length of the left front wing (cm)	length of the right front wing (cm)	expansion ratio of length for the front wing	length of the left hind wing (cm)	length of the right hind wing (cm)	expansion ratio of length for the hind wing
1	1.5	1.7	13.3%	0.9	1.0	11.1%
2	1.2	1.4	16.7%	0.8	0.9	12.5%
3	1.2	1.5	25%	0.9	0.9	0%
4	1.2	1.2	0%	0.8	1.0	25%
5	1.0	1.2	20%	0.8	0.9	12.5%
6	1.2	1.4	16.7%	0.8	0.8	0%

contained PY motifs, and nearly 30% contained various motifs that could be recognized by WW domains (Meng et al., 2015). The tandem WW domains of formin-binding protein 21 are connected by a highly flexible region, enabling their simultaneous interaction with two proline-rich motifs (Huang et al., 2009), therefore we suggest that the interaction of BmYki with its binding proteins was changed with the number of WW domains. Usually, alternative splicing has tissue specificity, expression patterns of *BmYki* isoforms also vary in the different tissues (Liang et al., 2018), so the size of different tissue may be regulated by different BmYki isoforms.

In the present study, we found that cell migration and cell proliferation could be facilitated by BmYki, the effectiveness of BmYki3 was greatest, followed by BmN-BmYki1, and BmN-BmYki2. Proteomic evidence suggested that the vast majority of genes have a single dominant splice isoform (Tress et al., 2016). Our previous study indicated that the expression level of BmYki3 was obviously higher than that of BmYki1 and BmYki2 overall (Liang et al., 2018), so BmYki3 may be a dominant splice isoform.

Cell migration could be promoted by Yap, a homolog of Drosophila Yki. In this study, we found that the migration of transformed cells could be promoted by overexpressing *BmYki*, the migration distance for Bm**N-B**mYki3 cells was the greatest, followed by Bm**N-BmYki1 and BmN-B**mYki2, indicating that BmYki isoforms facilitate cell migration and migration ability changes between BmYki isoforms.

The Hippo signaling pathway plays an important role in controlling the cell cycle, the size of cells and organs. In the silkworm, BmYki facilitates organ growth (Liu et al., 2016). Overexpression of BmYki1^{CA} in the posterior silk gland significantly increased the weight of the posterior silk gland (Zhang et al., 2017). Overexpression of BmYki1 in cultured *B. mori* embryonic cells indicated that the transcription of silk protein-coding genes and transcription factors regulating the synthesis of silk proteins were down-regulated remarkably (Zeng et al., 2017), suggesting that BmYki1 plays a role in controlling the size of silk glands and the expression of silk protein-coding genes. Knocking out BmYki led to reduced body size, molting defects, and eventually, larval lethality (Xu et al., 2018b). Somatic development and cell proliferation of the silkworm could be regulated by the Hippo pathway (Li et al., 2018). Our previous study showed that the wing size of silkworm was atrophied by silencing the BmYki gene and increased by overexpressing BmYki3 at day 3 of pupation (Liang et al., 2018). In the present study, we found that the wing size of the silkworm could be increased by overexpressing BmYki1 or BmYki2, and the proliferation, cell cycle, and size of cultured BmN cells could be facilitated by BmYki isoforms, suggesting that the organ is enlarged by virtue of its action on proliferation and/or size of the cell.

A previous study has indicated that upstream components Ex, Mer, Kibra, Crb, and Fj of the Hippo pathway are also targets of Yki, which provided a negative feedback mechanism to regulate the status of Hippo pathway precisely (Genevet et al., 2010). A similar result was found in this study, suggesting that the mechanism that regulates the status of the Hippo pathway is conserved.

It was reported that organ growth is also controlled by patterning signals including Wingless/Ints (Wnts), bone morphogenetic proteins (BMPs), and Hedgehogs (Hhs), and scaled by nutrient-dependent signals including insulin-like peptides (ILPs) transduced by the target of rapamycin (TOR) pathway (Parker and Struhl, 2015). Our results showed that the genes *Bmpr*, a negative regulator of TGF-β, and dpp, a member of the TGF-β superfamily, were both down-regulated by overexpressing *BmYki*, suggesting the TGF-β pathway could be regulated by the Hippo pathway. Moreover, it was reported that TGF-β can

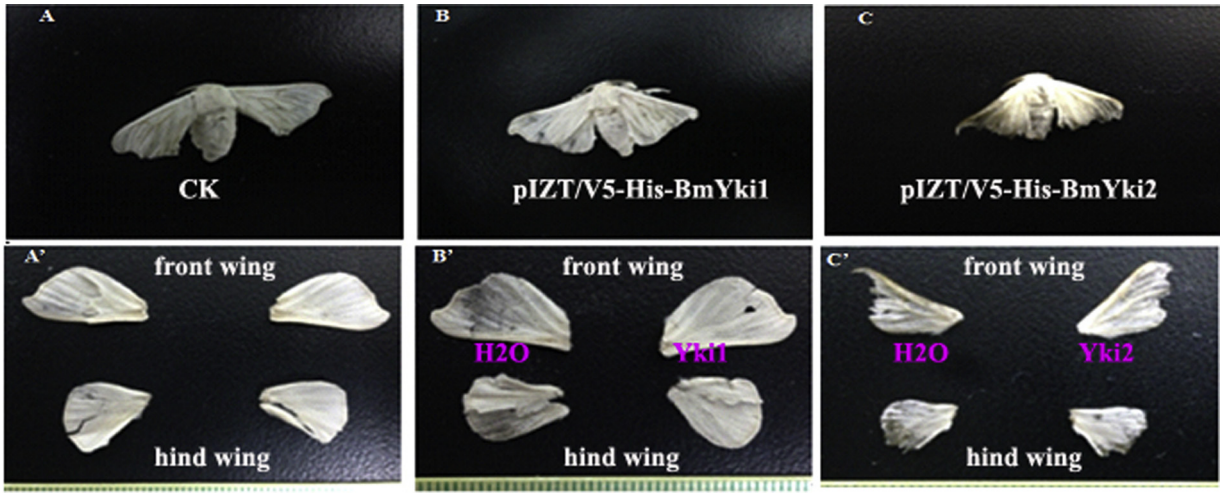

Fig. 8. Effects of up-regulating the *BmYki1* or *BmYki2* genes on wing disc development of pupae. A and A', normal moth wing. B and B', a moth which was injected with pIZT/V5-His-BmYki1 and water below the right and left wing disc, respectively, at day 3 of pupation; H2O, injected with water; Yki1, injected with pIZT/V5-His-BmYki1. C and C', a moth which was injected with pIZT/V5-His-BmYki2 and water below the right and left wing disc, respectively, at day 3 of pupation. H2O, injected with water; Yki2, injected with pIZT/V5-His-BmYki*2*.

target the Hippo pathway scaffold RASSF1A to facilitate YAP/SMAD2 nuclear translocation (Pefani et al., 2016), so there was a crosstalk between TGF-β and Hippo pathways. A recent study has indicated that knockdown of the junction component α-catenin caused nuclear accumulation and activation of YAP (Yki homolog) in mammalian cells (Yang et al., 2015). Our result showed that α-catenin gene expression level was down-regulated in the silkworm ovary-derived cultured cells where *BmYki*gene was upregulated, so we suggest the coadjustment of Yki and α-catenin. The expression level of Serr, a Notch ligand, was down-regulated in the transformed cells overexpressing *BmYki*, so the Hippo pathway cross-talks with Notch signaling (Kang et al., 2016) in the silkworm.

The Hippo pathway interacts with different growth pathways in distinct somatic cell types and interacts with the EGFR and JAK/STAT pathways to regulate the non-autonomous proliferation of germ cells, and plays an important role in establishing the precise balance of the soma and germ line (Sarikaya and Extavour, 2015). In the silkworm, the reduction of Yki expression by RNAi down-regulated Yki target genes in the ovary, decreased egg number (Liu et al., 2016) and Yorkie^{CA} overexpression in the posterior silk gland improves silk yield (Zhang et al., 2017). Our results indicated that the JAK-STAT signaling pathway could be down-regulated by overexpression of BmYki, suggesting that the Hippo pathway could regulate the precise balance of the soma and germ line. The JAK-STAT pathway is an important innate immune pathway. Recent results showed that YAP negatively regulated an antiviral immune response and YAP deficiency results in enhanced innate immunity (Wang et al., 2017). The JAK-STAT pathway has a more specialized role in the antiviral defense of silkworms (Zhang et al., 2016), therefore we speculate that the overexpression of *BmYki* may decrease the resistance to viral disease.

Acknowledgments

We gratefully acknowledge the financial support of the National Natural Science Foundation of China (31872424, 31272500), the National Basic Research Program of China (973 Program, 2012CB114600), and a project funded by the Priority Academic Program of Development of Jiangsu Higher Education Institutions.

Appendix A. Supplementary data

Supplementary material related to this article can be found, in the online version, at doi:https://doi.org/10.1016/j.biocel.2019.105599.

References

Madhuri, K.S., Amit, S., 2009. Regulation of organ size: insights from the Drosophila hippo signaling pathway. Dev. Dyn. 238, 1627–1637. https://doi.org/10.1002/dvdy.21996.

Stocker, H., Hafen, E., 2000. Genetic control of cell size. Curr. Opin. Genet. Dev. 10, 529–535. https://doi.org/10.1016/S0959-437X(00)00123-4.

Edgar, B.A., 2006. From cell structure to transcription: hippo forges a new path. Cell 124, 267–273. https://doi.org/10.1016/j.cell.2006.01.005.

Pan, D.J., 2007. Hippo signaling in organ size control. Genes Dev. 21, 886–897. https://doi.org/10.1101/gad.1536007.

Wu, S., Huang, J., Dong, J., Pan, D., 2003. Hippo encodes a Ste-20 family protein kinase that restricts cell proliferation and promotes apoptosis in conjunction with salvador and warts. Cell 114, 445–456. https://doi.org/10.1016/s0092-8674(03)00549-x.

Jia, J., Zhang, W., Wang, B., Trinko, R., Jiang, J., 2003. The Drosophila Ste20 family kinase dMST functions as a tumor suppressor by restricting cell proliferation and promoting apoptosis. Genes Dev. 17, 2514–2519. https://doi.org/10.1101/gad.1134003.

Harvey, K.F., Pfleger, C.M., Hariharan, I.K., 2003. The Drosophila Mst ortholog, hippo, restricts growth and cell proliferation and promotes apoptosis. Cell 114, 457–467. https://doi.org/10.1016/s0092-8674(03)00557-9.

Pantalacci, S., Tapon, N., Leopold, P., 2003. The Salvador partner Hippo promotes apoptosis and cell-cycle exit in Drosophila. Nat. Cell Biol. 5, 921–927. https://doi.org/10.1038/ncb1051.

Udan, R.S., Kango-Singh, M., Nolo, R., Tao, C., Halder, G., 2003. Hippo promotes proliferation arrest and apoptosis in the Salvador/Warts pathway. Nat. Cell Biol. 5, 914–920. https://doi.org/10.1038/ncb1050).

Lai, Z.C., Wei, X., Shimizu, T., Ramos, E., Rohrbaugh, M., Nikolaidis, N., Ho, L.L., Li, Y., 2005. Control of cell proliferation and apoptosis by mob as tumor suppressor, mats. Cell 120, 675–685. https://doi.org/10.1016/j.cell.2004.12.036.

Wei, X., Shimizu, T., Lai, Z.C., 2007. Mob as tumor suppressor is activated by Hippo kinase for growth inhibition in Drosophila. EMBO J. 26, 1772–1781. https://doi.org/10.1038/sj.emboj.7601630).

Qian, Y., Liu, J.B., Cao, G.L., Xue, R.Y., Gong, C.L., 2013. Cloning and sequence analysis of Hippo pathway related major genes of silkworm (Bombyx mori). Adv. Mat. Res. 796, 48–56. https://doi.org/10.1371/journal.pone.0182690.

Justice, R.W., Zilian, O., Woods, D.F., Noll, M., Bryant, P.J., 1995. The Drosophila tumor suppressor gene warts encodes a homolog of human myotonic dystrophy kinase and is required for the control of cell shape and proliferation. Genes Dev. 9, 534–546. https://doi.org/10.1101/gad.9.5.534.

Huang, J., Wu, S., Barrera, J., Matthews, K., Pan, D., 2005. The Hippo signaling pathway coordinately regulates cell proliferation and apoptosis by inactivating Yorkie, the Drosophila homolog of YAP. Cell 122, 421–434. https://doi.org/10.1016/j.cell.2005.06.007.

Ren, F., Zhang, L., Jiang, J., 2010. Hippo signaling regulates Yorkie nuclear localization and activity through 14-3-3 dependent and independent mechanisms. Dev. Biol. 337, 303–312. https://doi.org/10.1016/j.ydbio.2009.10.046.

Zhang, L., Ren, F., Zhang, Q., Chen, Y., Wang, B., Jiang, J., 2008. The TEAD/TEF family of transcription factor Scalloped mediates Hippo signaling in organ size control. Dev. Cell 14, 377–387. https://doi.org/10.1016/j.devcel.2008.01.006.

Goulev, Y., Fauny, J.D., Gonzalez-Marti, B., Flagiello, D., Silber, J., Zider, A., 2008. SCALLOPED interacts with YORKIE, the nuclear effector of the Hippo tumor-suppressor pathway in Drosophila. Curr. Biol. 18, 435–441. https://doi.org/10.1016/j.cub.2008.02.034.

Wu, S., Liu, Y., Zheng, Y., Dong, J., Pan, D., 2008. The TEAD/TEF family protein Scalloped mediates transcriptional output of the Hippo growth-regulatory pathway. Dev. Cell 14, 388–398. https://doi.org/10.1016/j.devcel.2008.01.007.

Zhao, B., Ye, X., Yu, J., Li, L., Li, W., Li, S., Yu, J., Lin, J.D., Wang, C.Y., Chinnaiyan, A.M., Lai, Z.C., Guan, K.L., 2008. TEAD mediates YAP-dependent gene induction and growth control. Genes Dev. 22, 1962–1971. https://doi.org/10.1101/gad.1664408.

Nolo, R., Morrison, C.M., Tao, C., Zhang, X., Halder, G., 2006. The bantam microRNA is a target of the Hippo tumor-suppressor pathway. Curr. Biol. 16, 1895–1904. https://doi.org/10.1016/j.cub.2006.08.057.

Thompson, B.J., Cohen, S.M., 2006. The Hippo pathway regulates the bantam microRNA to control cell proliferation and apoptosis in Drosophila. Cell 126, 767–774. https://doi.org/10.1016/j.cell.2006.07.013.

Campbell, S., Inamdar, M., Rodrigues, V., Raghavan, V., Palazzolo, M., Chovnick, A., 1992. The scalloped gene encodes a novel, evolutionarily conserved transcription factor required for sensory organ differentiation in Drosophila. Genes Dev. 6, 367–379. https://doi.org/10.1101/gad.6.3.367.

Xu, X., Bi, H.L., Zhang, Z.J., Yang, Y., Li, K., Huang, Y.P., Zhang, Y., He, L., 2018a. BmHpo mutation induces smaller body size and late stage larval lethality in the silkworm, Bombyx mori. Insect Sci. 25, 1006–1016. https://doi.org/10.1111/1744-7917.12607.

Li, N., Tong, X., Zeng, J., Meng, G., Sun, F., Hu, H., Song, J., Lu, C., Dai, F., 2018. Hippo pathway regulates somatic development and cell proliferation of silkworm. Genomics. https://doi.org/10.1016/j.ygeno.2018.02.014. S0888-7543 (18) 30122-8.

Zeng, W., Liu, R., Zhang, T., Zuo, W., Ou, Y., Tang, Y., Xu, H., 2018. BmYki is transcribed into four functional splicing isoforms in the silk glands of the silkworm, Bombyx mori. Gene 646, 39–46. https://doi.org/10.1016/j.gene.2017.12.047).

Liu, S., Zhang, P., Song, H.S., Qi, H.S., Wei, Z.J., Zhang, G., Zhan, S., Liu, Z., Li, S., 2016. *Yorkie* facilitates organ growth and metamorphosis in Bombyx. Int. J. Biol. Sci. 12, 917–930. https://doi.org/10.7150/ijbs.14872).

Zhang, P., Liu, S., Song, H.S., Zhang, G., Jia, Q., Li, S., 2017. Yorkie ^{CA} overexpression in the posterior silk gland improves silk yield in Bombyx mori. J. Insect Physiol. 100, 93–99. https://doi.org/10.1016/j.jinsphys.2017.06.001).

Xu, X., Zhang, Z., Yang, Y., Huang, S., Li, K., He, L., Zhou, X., 2018b. Genome editing reveals the function of Yorkie during the embryonic and early larval development in silkworm, Bombyx mori. Insect Mol. Biol. 27, 675–685. https://doi.org/10.1111/imb.12502).

Liang, Z., Lu, Y., Qian, Y., Zhu, L., Kuang, S., Chen, F., Feng, Y., Hu, X., Cao, G., Xue, R., Gong, C., 2018. Cultured cells and wing disc size of silkworm can be controlled by the Hippo pathway. Open Biol. 8, 180029. https://doi.org/10.1098/rsob.180029.

Bates, D.O., Morris, J.C., Oltean, S., Donaldson, L.F., 2017. Pharmacology of modulators of alternative splicing. Pharmacol. Rev. 69, 63–79. https://doi.org/10.1124/pr.115.011239.

Garfinkel, M.D., Wang, J., Liang, Y., Mahowald, A.P., 1994. Multiple products from the shavenbaby-ovo gene region of Drosophila melanogaster: relationship to genetic complexity. Mol. Cell. Biol. 14, 6809–6818. https://doi.org/10.1128/mcb.14.10.6809.

Lee, S., Garfinkel, M.D., 2000. Characterization of Drosophila OVO protein DNA binding specificity using random DNA oligomer selection suggests zinc finger degeneration. Nucleic Acids Res. 28, 826–834. https://doi.org/10.1093/nar/28.3.826.

Chen, H.I., Sudol, M., 1995. The WW domain of Yes-associated protein binds a proline-rich ligand that differs from the consensus established for Src homology 3-binding modules. Proc. Natl. Acad. Sci. 92, 7819–7823. https://doi.org/10.1073/pnas.92.17.7819.

Oh, H., Irvine, K.D., 2009. In vivo analysis of Yorkie phosphorylation sites. Oncogene 28, 1916–1927. https://doi.org/10.1038/onc.2009.43.

Tress, M.L., Martelli, P.L., Frankish, A., Reeves, G.A., Wesselink, J.J., Yeats, C., Olason, P.I., Albrecht, M., Hegyi, H., Giorgetti, A., Raimondo, D., Lagarde, J., Laskowski, R.A., López, G., Sadowski, M.I., Watson, J.D., Fariselli, P., Rossi, I., Nagy, A., Kai, W., Størling, Z., Orsini, M., Assenov, Y., Blankenburg, H., Huthmacher, C., Ramírez, F.,

Schlicker, A., Denoeud, F., Jones, P., Kerrien, S., Orchard, S., Antonarakis, S.E., Reymond, A., Birney, E., Brunak, S., Casadio, R., Guigo, R., Harrow, J., Hermjakob, H., Jones, D.T., Lengauer, T., Orengo, C.A., Patthy, L., Thornton, J.M., Tramontano, A., Valencia, A., 2007. The implications of alternative splicing in the ENCODE protein complement. Proc. Natl. Acad. Sci. U.S.A. 104, 5495–5500. https://doi.org/10.1073/pnas.0700800104.

Oh, H., Irvine, K.D., 2008. In vivo regulation of Yorkie phosphorylation and localization. Development 135, 1081–1088. https://doi.org/10.1242/dev.015255.

Colak, R., Kim, T., Michaut, M., Sun, M., Irimia, M., Bellay, J., Myers, C.L., Blencowe, B.J., Kim, P.M., 2013. Distinct types of disorder in the human proteome: functional implications for alternative splicing. PLoS Comput. Biol. 9, e1003030. https://doi.org/10.1371/journal.pcbi.1003030.

Meng, G., Dai, F., Tong, X., Li, N., Ding, X., Song, J., Lu, C., 2015. Genome-wide analysis of the WW domain-containing protein genes in silkworm and their expansion in eukaryotes. Mol. Genet. Genom. 290, 807–824. https://doi.org/10.1007/s00438-014-0958-6.

Huang, X., Beullens, M., Zhang, J., Zhou, Y., Nicolaescu, E., Lesage, B., Hu, Q., Wu, J., Bollen, M., Shi, Y., 2009. Structure and function of the two tandem WW domains of the pre-mRNA splicing factor FBP21 (formin-binding protein 21). J. Biol. Chem. 284, 25375–25387. https://doi.org/10.1074/jbc.M109.024828.

Tress, M.L., Abascal, F., Valencia, A., 2016. Alternative splicing may not be the key to proteome complexity. Trends Biochem. Sci. 42, 98–110. https://doi.org/10.1016/j.tibs.2016.08.008.

Zeng, W., Wang, R., Zhang, T., Gong, C., Zuo, W., Liu, R., Ou, Y., Xu, H., 2017. Cloning and expression analysis of BmYki gene in silkworm, Bombyx mori. PLoS One 12, e0182690. https://doi.org/10.1371/journal.pone.0182690).

Genevet, A., Wehr, M.C., Brain, R., Thompson, B.J., Tapon, N., 2010. Kibra is a regulator of the Salvador/Warts/Hippo signaling network. Dev. Cell 18, 300–308. https://doi.org/10.1016/j.devcel.2009.12.011.

Parker, J., Struhl, G., 2015. Scaling the Drosophila wing: TOR-dependent target gene access by the Hippo pathway transducer Yorkie. PLoS Biol. 13, e1002274. https://doi.org/10.1371/journal.pbio.1002274).

Pefani, D.E., Pankova, D., Abraham, A.G., Grawenda, A.M., Vlahov, N., Scrace, S., O' Neill, E., 2016. TGF-β targets the Hippo pathway scaffold RASSF1A to facilitate YAP/SMAD2 nuclear translocation. Mol. Cell 63, 156–166. https://doi.org/10.1016/j.molcel.2016.05.012.

Yang, C.C., Graves, H.K., Moya, I.M., Tao, C., Hamaratoglu, F., Gladden, A.B., Halder, G., 2015. Differential regulation of the Hippo pathway by adherens junctions and apical–basal cell polarity modules. Proc. Natl. Acad. Sci. U.S.A. 112, 1785–1790. https://doi.org/10.1073/pnas.1420850112.

Kang, W., Cheng, A.S., Yu, J., To, K.F., 2016. Emerging role of Hippo pathway in gastric and other gastrointestinal cancers. World J. Gastroenterol. 22, 1279–1288. https://doi.org/10.3748/wjg.v22.i3.1279.

Sarikaya, D.P., Extavour, C.G., 2015. The Hippo pathway regulates homeostatic growth of stem cell niche precursors in the Drosophila ovary. PLoS Genet. 11, e1004962. https://doi.org/10.1371/journal.pgen.1004962.5.

Wang, S., Xie, F., Chu, F., Zhang, Z., Yang, B., Dai, T., Gao, L., Wang, L., Ling, L., Jia, J., van Dam, H., Jin, J., Zhang, L., Zhou, F., 2017. Corrigendum: YAP antagonizes innate antiviral immunity and is targeted for lysosomal degradation through IKKε-mediated phosphorylation. Nat. Immunol. 18, 1270. https://doi.org/10.1038/ni.3744.

Zhang, X., Guo, R., Kumar, D., Ma, H., Liu, J., Hu, X., Cao, G., Xue, R., Gong, C., 2016. Identification, gene expression and immune function of the novel Bm-STAT gene in virus-infected Bombyx mori. Gene 577, 82–88. https://doi.org/10.1016/j.gene.2015.11.027.